Structures, Spectra, and Energies of Niobium Clusters from Nb−13 to Nb−20

ARTICLE *in* THE JOURNAL OF PHYSICAL CHEMISTRY A · JUNE 2012

Impact Factor: 2.69 · DOI: 10.1021/jp302279j · Source: PubMed

2 AUTHORS, INCLUDING:

Minh Tho Nguyen
University of Leuven
748 PUBLICATIONS **10,856** CITATIONS

SEE PROFILE

THE JOURNAL OF PHYSICAL CHEMISTRY A

Article

pubs.acs.org/JPCA

Structures, Spectra, and Energies of Niobium Clusters from Nb_{13} to Nb_{20}

Pham Vu Nhat[†,‡] and Minh Tho Nguyen*[,†,§]

[†]Department of Chemistry, University of Leuven, B-3001 Leuven, Belgium

[‡]Department of Chemistry, Can Tho University, Can Tho, Vietnam

[§]Institute for Computational Science and Technology (ICST), HoChiMinh City, Vietnam

Supporting Information

ABSTRACT: A comprehensive theoretical investigation on structures and properties of niobium clusters in the range from 13 to 20 atoms, in three different charged states, is performed by using the BPW91 and M06 functionals and the cc-pVDZ-PP basis set. These species are predicted to prefer low spin ground state, i.e., singlet (for even electron) and doublet (for odd electron) systems. In terms of growth mechanism, a compact structure with one Nb encapsulated by a cage formed from five and six triangles is found to be favored over an icosahedral evolution. Unlike many 3d metals, whose volumes are much smaller, 13 and 19 Nb atoms clusters do not exist as icosahedra and double-icosahedra. A distinct case is Nb_{15} as it bears a slightly distorted bcc structure. For some systems, several lower lying isomers are computed to be so close in energy that DFT computations cannot clearly establish their ground electronic states. The existence of structural isomers with comparable energy content is established for Nb_n species with n = 13, 18, 19, and 20 in both neutral and charged states. The vibrational (IR) spectra are also calculated. While the spectra of smaller systems are strongly dependent on addition or removal of an electron from the neutral, the spectra of the larger size clusters are mostly independent of the charged state. The neutrals and their corresponding ions usually have a quite similar IR pattern. Electron affinities (EA), ionization energies (IE), average binding energies, dissociation energies, and frontier orbital energy gaps are evaluated. The computed EAs and IEs are generally in fair agreement with experiment. The Nb_{15} system is observed to be stable and it can form a highly symmetric structure in all charged states with both open and closed electron shells.

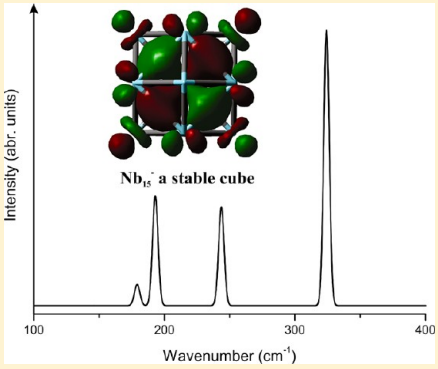

1. INTRODUCTION

The studies in the clusters of the elements have grown exponentially in recent time, motivated by both fundamental interest and practical applications.[1,2] Indeed, the deep knowledge on molecular and electronic structures constitutes an initial step in any attempt of understanding and interpreting the experimental observations on the thermal, optical, magnetic, and catalytic properties of nanoparticles. Compared with other transition metals, in particular the coinage metals, relatively fewer studies have been devoted to clusters of niobium by both experiment and theory. Early spin-polarized DFT calculations[3,4] for Nb_n clusters containing up to n = 10 suggested that these species prefer the lowest possible spin state, except for Nb_2, and a close-packed growth behavior. Magnetic deflection experiments on neutral clusters also confirmed an antiferromagnetic ground state with S = 0 for all even sized systems considered.[5]

The compact growth mechanism and the preference for the low-spin configurations were also observed for niobium clusters in a subsequent DFT study.[6] Recent studies[7] in addition pointed out the existence of structural isomerism for 6, 9, and 12 Nb atom systems, which was suggested in an earlier study on N_2 and D_2 reaction kinetics.[8] The structural isomers of transition metal clusters are usually very close in energy, leading to considerable challenges for both theory and experiment to identify their global minima. In these cases, information obtained from both approaches is necessary. One of the more reliable determinations involves a comparison of the measured IR spectra to those computed for different isomers, as the vibrational spectroscopy is particularly sensitive to the internal atomic arrangement.[9] Fielicke and co-workers[10,11] were able to record the vibrational spectra for both neutral and cationic $Nb_n^{0/+}$ clusters with n = 5–12, but no experimental IR data are reported yet for larger species, n > 12 atoms.

The reactivities of neutral Nb_n toward small molecules such as H_2, N_2, and CO showed a rather interesting and simple pattern: even-numbered systems, such as Nb_8, Nb_{10}, and Nb_{16}, are significantly less reactive than odd-numbered counterparts.[12,13] Regarding the cationic clusters, the difference between the sizes is on the contrary not significant, and their reactivities are apparently size-independent.[14−16] From the photoelectron spectra recorded by using a laser vaporization technique, Kietzmann et al.[17] determined the vertical detachment energies

Received: March 8, 2012
Revised: June 9, 2012
Published: June 11, 2012

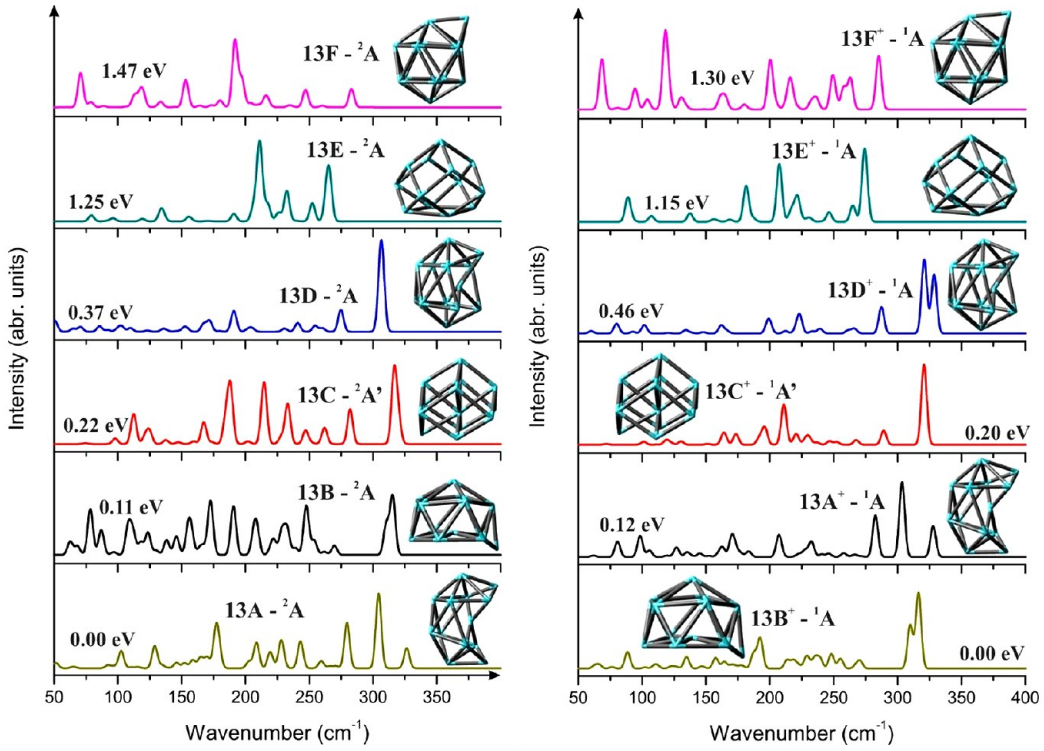

Figure 1. Predicted IR spectra of Nb_{13} neutral (left) and cation (right).

(VDE) for niobium cluster anions containing from 3 to 25 atoms. The ionization energies for a large number of neutral Nb_n (n = 2−76) clusters were also measured by using the photoionization efficiency (PIE) technique.[18] These investigations on ionization energies and electron affinities pointed out even−odd oscillations for clusters in the size range of 6−17 atoms. Along the curve of ionization energy values as a function of the size, local maxima have experimentally been seen at n = 8, 10, and 16. Such cluster sizes were also predicted to have larger frontier orbital energy gaps than their neighbors. Recently, Nb_{10} was predicted to be particularly stable, having a spherically aromatic character, high chemical hardness, and large HOMO−LUMO gap.[7] However, there is not much reliable information on Nb_{16} and, more generally, on the systems larger than Nb_{12}. Many aspects of these clusters are still not well established, and thus insights into their basic properties should be helpful not only to review the prior experimental findings but also to provide useful predictions for future experiments.

In our continuing theoretical studies on Nb_n clusters, we have considered their size from n = 2 to 12.[7] We now extend the work dealing with the structural, electronic, energetic, and vibrational properties of neutral and singly charged $Nb_n^{0/\pm}$ compounds in the larger range from the tridecamer (n = 13) to the eicosamer (n = 20). First we report the results of geometrical and electronic structures, along with their growth behavior. As for a prediction, some spectroscopic features of the ground state and lower lying states are also presented. The calculations of dissociation energies (D_e), binding energies per atom (BE), electron affinities (EA), and ionization energies (IE) as a function of cluster size are then determined and used to rationalize available experimental data. The main purpose of this study is thus to complete the predictions on the lowest energy structures for the whole range from n = 2 to 20, and thereby to emphasize the general trends in size-dependent growth.

2. COMPUTATIONAL METHODS

All quantum chemical calculations are carried out with the Gaussian 09 suite of programs.[19] The neutral clusters Nb_n with n = 13−20 are initially investigated by making use of a GGA functional, namely BPW91,[20] and the LanL2DZ basis set.[21] Subsequently, geometries of the most relevant lower-lying isomers are reoptimized by utilizing the correlation-consistent cc-pVDZ-PP basis set.[22] These basis sets take the 4s, 4p, 4d, 5s, and 5p orbitals of the Nb atom as valence orbitals. The electrons in the inner shells along with the nucleus are considered as the inert core. The interaction between valence electrons and the inert core is included in the pseudopotential (PP), which already includes the relativistic effects that are crucial in the treatment of heavy elements.

For each size, we consider the two lowest spin states as magnetic deflection experiments revealed that Nb clusters exhibit an antiferromagnetic ground state with S = 0.[5] In order to estimate the EAs and IEs, we furthermore explore the optimal structures for the anionic Nb_n^- and cationic Nb_n^+ clusters having the same sizes (n = 13−20), using the same level, namely the BPW91 functional in conjunction with the cc-pVDZ-PP basis set. The accuracy of such a computational approach in predicting molecular properties for Nb clusters has been evaluated in our recent work.[7] Other thermochemical properties including atomization and dissociation energies are computed by employing the hybrid meta-GGA M06 functional, which appears to be more reliable than the pure GGA BPW91. The calculations at the M06/cc-pVDZ-PP level are performed on the basis of the BPW91/cc-pVDZ-PP optimized geometries. Overall, error bars of ±0.3 eV can be expected on the calculated energetic parameters.

The structures considered for initial optimizations are constructed by using two different routes. In the first one, the initial geometries of a certain size Nb_n are generated from the

dx.doi.org/10.1021/jp302279j | J. Phys. Chem. A 2012, 116, 7405−7418

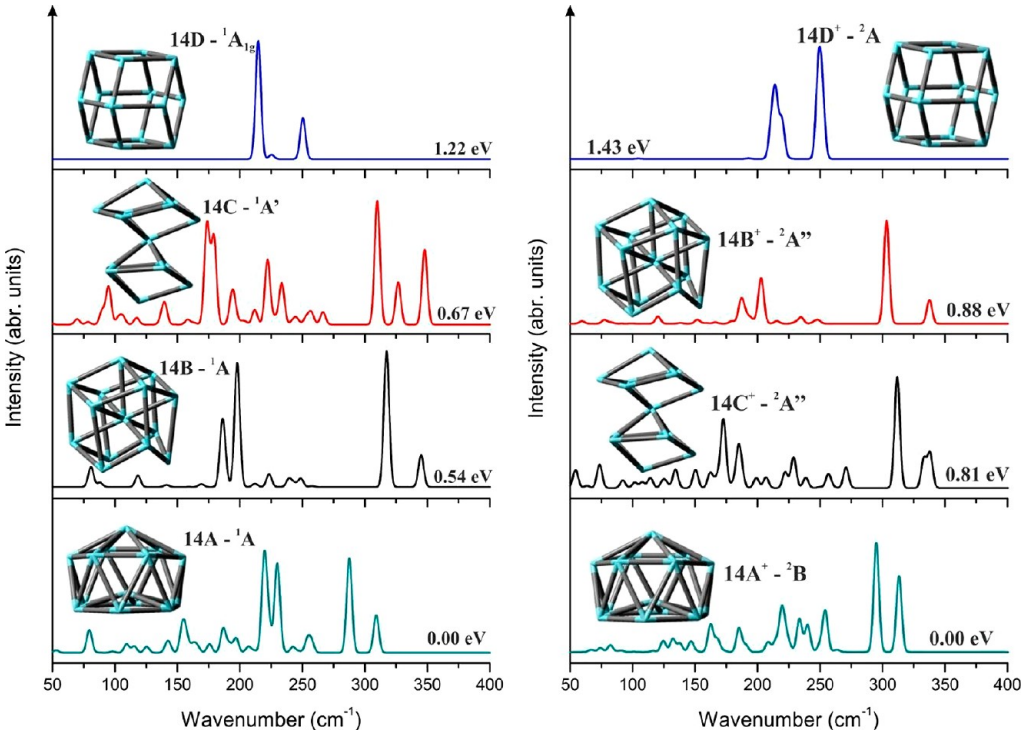

Figure 2. Predicted IR spectra of Nb_{14} neutral (left) and cation (right).

lowest lying isomers of the smaller size Nb_{n-1} by adding an extra Nb atom systematically at all possible positions. This procedure can also be called a successive growth algorithm.[23] In the second route, we employ the reported results of other transition metal clusters at similar sizes as a guide. Harmonic vibrational frequencies are also computed to confirm that the optimized geometries correspond to local minima or transition states on the potential energy surface, and more importantly to simulate their vibrational spectra (without scaling). Though, to our best knowledge, the experimental IR spectra for clusters containing more than 12 Nb atoms have not been published so far; they are reported here as predictions that may allow the optimal structures to be verified when the relevant spectroscopic information is available.

3. RESULTS AND DISCUSSION

We first discuss the properties of the Nb_n clusters considered in three different charged states. An analysis of the growth trends with respect to the cluster size is presented in subsequent sections.

3.1. Structures and Vibrational Spectra. *The Tridecamers Nb_{13}.* Relevant structures are displayed in Figure 1. Although an icosahedral shape is found to be the lowest energy isomer for several 13-atom 4d transition-metal clusters such as Y, Zr, and Pd,[24] this form is not even a local minimum for Nb_{13}. A severely distorted icosahedron similar to **13B** was proposed as the lowest energy form of Nb_{13}.[25] Two isomers **13A** and **13B**, which can be considered as degenerate with an energy gap of 0.1 eV, an amount lying within the error bars of the DFT methods employed (see above), are found to compete for the ground state. Both have a low-spin ^2A (C_1) ground state. Other isomers, namely **13C**, **13D**, **13E**, and **13F** (Figure 1), are located from 0.22 to 1.47 eV above **13A**.

Following electron detachment or attachment, the forms **13A** and **13B** are also giving rise to the most stable configurations for Nb_{13}^+ and Nb_{13}^- as well. However, in these ions, the resulting **13A**$^+$ is 0.12 eV higher in energy than the **13B**$^+$, while the anion **13A**$^-$ is predicted to be 0.32 eV more stable than the counterpart **13B**$^-$. Such energy difference remains small to allow a definitive assignment for the global minimum to be made.

As shown in Figure 1, the spectroscopic signatures of **13A** contain the highest energy band centered at ~330 cm^{-1} and the highest intensity peak at around 300 cm^{-1}. The IR spectrum of the isoenergetic isomer **13B** is more complex with the most significant peak at ~320 cm^{-1} and some in the vicinity below 250 cm^{-1}. Though both the neutral and cation seem to have a similar spectral pattern, there still exist some minor but typical differences between their spectral lines. The spectra of **13A**$^+$ and **13B**$^+$ are in fact much smoother than those of **13A** and **13B**.

The calculated spectra for some lower-lying states of the anion are plotted in Figure S1 of the Supporting Information (ESI). Both **13A**$^-$ and **13B**$^-$ isomers are predicted to vibrate in a range below 320 cm^{-1} with the appearance of a high-frequency band above 300 cm^{-1} related to the encapsulated atom.

The Tetradecamers Nb_{14}. Related structures are given in Figure 2. A previous study[6] revealed that the global minimum of Nb_{14} can be described as a hexagonal antiprism with an atom situated at the center and one face capped (cf. **14A** in Figure 2). Our findings concur with this, and demonstrate in addition that such a shape turns out to be the energetically optimized configuration for both the cation Nb_{14}^+ and anion Nb_{14}^-.

14A exhibits a particularly high stability as compared to other structures detected for Nb_{14}. For example, an incomplete cubic with one encapsulated atom **14B** is computed at 0.54 eV above the ground state ^1A of **14A**. Niobium clusters apparently do not favor icosahedral form as a capped icosahedron is not even a local minimum of the 14-atom system.

The vibrational spectrum of the neutral ground state **14A** (^1A) covers the range below 325 cm^{-1} with five specific peaks in the vicinity of 200−325 cm^{-1}. As in the 13-atom system, the IR

dx.doi.org/10.1021/jp302279j | J. Phys. Chem. A 2012, 116, 7405−7418

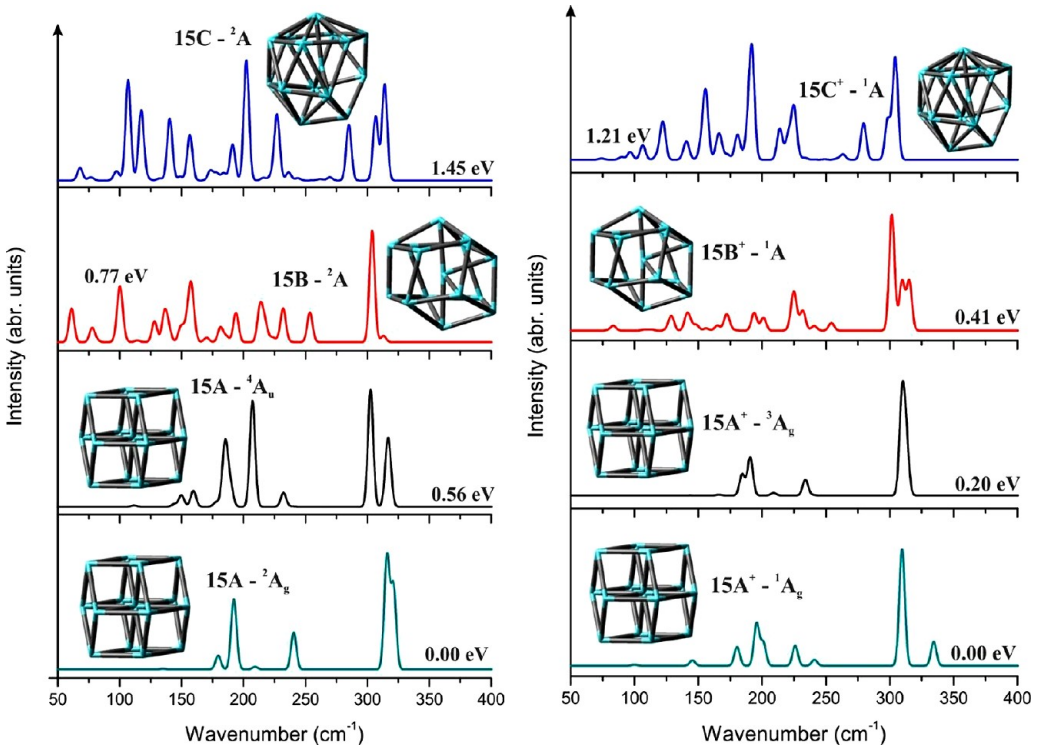

Figure 3. Predicted IR spectra of Nb_{15} neutral (left) and cation (right).

spectrum of this species is not much changed following the removal of an electron from the neutral. We actually observe a similarity in the band pattern of the cation spectrum. However, the intensities of some bands located around 225 cm^{-1} are now substantially reduced, in addition to a small blue shift. The spectrum of the anion in its ground state **14A**$^-$ structure (Figure S1, ESI) is somewhat distinguishable from that of **14A**.

The Pentadecamers Nb$_{15}$. Kietzmann et al.[17] predicted that the appearance of a bulk-like bcc structure may occur at Nb_{15}^-. Besides, upon electron detachment from the anion Nb_n^- the atomic arrangement remains almost unchanged,[7] so the neutral Nb_{15} is expected to involve a geometric bcc shell closing as well. In fact, we find a rhombic dodecahedron (structure **15A** in Figure 3) to be the most stable form of Nb_{15}. Because of a Jahn−Teller distortion, the cluster prefers to exist in a low C_i symmetry (^2A_g state), rather than in a perfectly cubic shape (O_h). Other isomers include a capped hexagonal antiprism structure **15B**, and an incomplete Frank−Kasper structure **15C**, both having significantly higher energy content (0.77−1.45 eV).

The lowest energy isomer of the cationic state Nb_{15}^+ is also the distorted cube (C_i), while that of the anion Nb_{15}^- corresponds to a regular cube (O_h). Again, both Nb_{15}^+ and Nb_{15}^- ions prefer to exist respectively in low spin ^1A_g and $^1A_{1g}$ states. For the cation, the ^1A_g state is ∼0.2 eV lower than the ^3A_g. The energy separations of other states to the ground state can be found in Table 1. The HOMO of **15A**$^-$ is triply degenerate, so removing either one or two electrons to form respectively the neutral **15A** and the cation **15A**$^+$ is accompanied by symmetry reduction from O_h to C_i. Overall, the Nb_{15} clusters can be regarded as the capped cubes irrespective of their charged state.

Figure 3 shows the IR spectra computed for some lower-lying states of the 15-atom clusters. The calculated spectra of both neutral and cationic ground states **15A** (^2A_g) and **15A**$^+$ (^1A_g) contain the most intense band between 310 and 325 cm^{-1}, besides several peaks in the vicinity of 175−250 cm^{-1}. However, they can still be distinguished from each other. In fact, while the neutral is predicted to vibrate below 325 cm^{-1}, a relatively distinct peak around 335 cm^{-1} is seen on the IR pattern of **15A**$^+$. The predicted vibrational spectra of anionic species are displayed in Figure S1 of the ESI. The spectrum of the ground state **15A**$^-$ structure is characterized by four triplets located at around 320, 240, 190, and 180 cm^{-1}.

The Hexadecamers Nb$_{16}$. According to Kumar and Kawazoe,[6] the lowest energy isomer of Nb_{16} can be described as an hexagonal antiprism with one side capped by two atoms and the other side capped by a single atom. Our results concur with this finding, and demonstrate in addition that such a shape **16A** (Figure 4) turns out to be the energetically optimized configuration not only for Nb_{16} but also for its singly charged states Nb_{16}^+ and Nb_{16}^-.

16A is a Frank−Kasper polyhedron that has 15 vertexes and all triangular faces. Note that a vertex that is the meeting of N faces is called the N-degree vertex, or the vertex having a degree of N (5-faces stands for 5 triangular faces). Accordingly, among the vertexes of **16A**, 12 vertexes are the meetings of 5 triangular faces, whereas the 3 remaining vertexes are the meetings of 6 triangular faces. **16A** conformation can thus be viewed as a (12,3) Frank−Kasper (FK) polyhedron. However, this 15-vertex FK with three 6-degree vertices has a D_3 point group rather than a perfect D_{3h} deltahedron, whose faces are all equilateral triangles.

The isomer **16B**, which is very similar to **16A** only the atom surrounded by 15 other atoms is not at the central position, is 0.6 eV higher in energy.

Capping of the 15-atom cubic structure yields isomer **16C**, which is 1.61 eV above **16A**. Relative energies of the cationic and anionic states are listed in Table 1.

The computed IR spectra of some lower lying states of Nb_{16} and Nb_{16}^+ are shown in Figure 4. For all states, the vibrational fundamentals appear below 325 cm^{-1}. The spectrum of the neutral ground ^1A state exhibits an intense peak at 310 cm^{-1}, and

dx.doi.org/10.1021/jp302279j | J. Phys. Chem. A 2012, 116, 7405−7418

Table 1. Ground and Lower Lying States of $Nb_n^{0/\pm}$ (n = 13−17) Clusters and Their Relative Energies (RE, eV, BPW91/cc-pVDZ-PP)

cluster	structure	state	RE (eV)	cluster	structure	state	RE (eV)
Nb_{13}	**13A** (C_1)	^{2}A	0.00	Nb_{15}	**15C** (C_1)	^{2}A	1.45
	13B (C_1)	^{2}A	0.11	Nb_{15}^+	**15A**$^+$ (C_i)	^1A_g	0.00
	13C (C_s)	^{2}A′	0.22			^3A_g	0.20
	13D (C_1)	^{2}A	0.37		**15B**$^+$ (C_1)	^{1}A	0.41
	13E (C_1)	^{2}A	1.25		**15C**$^+$ (C_1)	^{1}A	1.21
	13F (C_1)	^{2}A	1.37	Nb_{15}^-	**15A**$^+$ (C_i)	^1A_g	0.00
Nb_{13}^+	**13A**$^+$ (C_1)	^{1}A	0.12			^3A_g	0.35
	13B$^+$ (C_1)	^{1}A	0.00		**15B**$^+$ (C_2)	^{1}A	1.25
	13C$^+$ (C_s)	^{1}A′	0.20		**15C**$^+$ (C_1)	^{1}A	1.70
	13D$^+$ (C_1)	^{1}A	0.46	Nb_{16}	**16A** (D_3)	^{1}A	0.00
	13E$^+$ (C_1)	^{1}A	1.15		**16B** (C_1)	^{1}A	0.60
	13F$^+$ (C_1)	^{1}A	1.30		**16C** (C_1)	^{1}A	1.61
Nb_{13}^-	**13A**$^-$ (C_1)	^{1}A	0.00		**16D** (C_3)	^{1}A	2.70
	13B$^-$ (C_1)	^{1}A	0.34	Nb_{16}^+	**16A**$^+$ (C_1)	^{2}A	0.00
	13C$^-$ (C_s)	^{1}A′	0.36		**16B**$^+$ (C_1)	^{2}A	0.26
	13D$^-$ (C_1)	^{1}A	1.31		**16C**$^+$ (C_1)	^{2}A	1.68
	13E$^-$ (C_1)	^{1}A	1.45		**16D**$^+$ (C_3)	^{2}A	2.90
	13F$^-$ (C_1)	^{1}A	1.57	Nb_{16}^-	**16A**$^-$ (C_2)	^{2}A	0.00
Nb_{14}	**14A** (C_{2v})	$^1A_1$	0.00		**16B**$^-$ (C_1)	^{2}A	0.46
	14B (C_1)	^{1}A	0.54		**16C**$^-$ (C_1)	^{2}A	1.53
	14C (C_s)	^{1}A′	0.67		**16D**$^-$ (C_3)	^{2}A	2.58
	14D (O_h)	$^1A_{1g}$	1.22	Nb_{17}	**17A** (C_1)	^{2}A	0.00
Nb_{14}^+	**14A**$^+$ (C_2)	^{2}B	0.00		**17B** (C_2)	^{2}A	0.45
	14B$^+$ (C_s)	^{2}A″	0.88		**17C** (C_1)	^{2}A	1.51
	14C$^+$ (C_s)	^{2}A″	0.81		**17D** (C_i)	^2A_u	1.81
	14D$^+$ (C_1)	^{2}A	1.43	Nb_{17}^+	**17A**$^+$ (C_1)	^{1}A	0.00
Nb_{14}^-	**14A**$^-$ (C_{2v})	$^2A_2$	0.00		**17B**$^+$ (C_1)	^{1}A	0.50
	14B$^-$ (C_1)	^{2}A	0.62		**17C**$^+$ (C_{3v})	$^1A_1$	1.60
	14C$^-$ (C_s)	^{2}A′	0.70		**17D**$^+$ (C_i)	^1A_g	1.69
	14D$^-$ (O_h)	$^2B_{2g}$	1.62	Nb_{17}^-	**17A**$^-$ (C_1)	^{1}A	0.00
Nb_{15}	**15A** (C_i)	^2A_g	0.00				
	17B$^-$ (C_1)	^{1}A	0.57				
		^4A_u	0.56		**17C**$^-$ (C_1)	$^1A_1$	1.40
	15B (C_2)	^{2}A	0.77		**17D**$^-$ (C_i)	^1A_g	1.95

some lower intensity peaks below 300 cm^{-1}. The spectrum of the ^{2}A ground state of **16A**$^+$ is characterized by a doublet at ∼305 cm^{-1}. In addition, five distinct peaks are present in the range 100−300 cm^{-1}.

As shown in Figure S1 of the ESI, at least four distinct absorption bands can be found in the range below 300 cm^{-1} on the vibrational spectrum of the ^{2}A anion ground state of **16A**$^-$.

The Heptadecamers Nb_{17}. We identify several possible low-lying structures for Nb_{17} including **17A**, **17B**, **17C**, and **17D** displayed in Figure 5. Among them, the distorted (12,4) FK **17A**, having no symmetry and a low-spin electronic state, is found to be the global minimum of Nb_{17} and also for its ions $Nb_{17}^{\pm}$. In the case of 17-atom systems, a regular FK polyhedron, i.e., a 16-vertex tetracapped truncated tetrahedron (T_d symmetry), is not an energetically preferred conformation. Previously, an isomer obtained from **16A** by adding one Nb atom (see structure **17C**) has been predicted to be the most stable form for Nb_{17}.[6] However, in the present study, **17C** (^{1}A) is computed to lie around 1.5 eV above **17A** (^{1}A). Another isomer **17B**, which is very similar to **17A** but more symmetric (C_2), is located 0.45 eV above. The 17-atom species can also appear as a heptagonal antiprism with each heptagonal face capping one atom (see structure **17D**), but such a local minimum is much less stable than **17A**, being separated by 1.8 eV.

The spectra of 17-atom species are also faintly dependent on the removal of an electron from the neutral. Both Nb_{17} and Nb_{17}^+ are predicted to exhibit in ground state a typical peak around 280 cm^{-1} on their IR spectra. An interesting point here is that they vibrate at a considerably lower energy than the smaller size $Nb_{13}^{0/+}$−$Nb_{16}^{0/+}$ clusters. As compared to **17A** (^{2}A), the closed-shell counterpart **17A**$^+$ (^{1}A) has a somewhat smoother spectrum as it is likely to be more symmetric. There also exist some typical bands as spectroscopic signatures of the ^{1}A anion ground state at ∼280 cm^{-1}, besides several lower intensity bands in the range below 240 cm^{-1} (cf. Figure S1 of the ESI).

The Octadecamers Nb_{18}. Our previous studies[7] show that the optimal Nb clusters prefer a close-packed growth behavior rather than a successive growth pattern. This also holds true for the 18-atom species. In fact, the isomer obtained from **17A** by adding an extra Nb atom (cf. structure **18C**) is computed to be around 0.54 eV higher in energy than the compact **18A**. The latter is also derived from five and six faces, but it is not a FK polyhedron because it has two pairs of adjacent degree six vertices. Only deltahedra with degree 5 and 6 vertices and with no adjacent degree 6 vertices are considered as FK polyhedra.[26]

A 2-fold symmetry isomer **18B**, being 0.25 eV higher in energy than **18A**, is obtained when one top-side atom is cut from the lowest energy of the larger size **19A**.

Following electron detachment and attachment, the two shapes **18A** and **18B** are also giving rise to the energetically optimized configurations **18A**$^+$ and **18B**$^+$ for Nb_{18}^+ and **18A**$^-$ and **18B**$^-$ for Nb_{18}^-. Isomers **18B**$^+$ and **18B**$^-$ are now found to lie 0.36 and 0.10 eV higher in energy than **18A**$^+$ and **18A**$^-$, respectively. In previous investigations on clusters of Fe, Ca, and Sr,[27,28] global minima for the 18-atom systems are related to a double icosahedron by removal of one atom. In the present study, such a form **18D** (Figure 6) with D_{5h} symmetry and a low-spin $^1A_1'$ state remains a local minimum, but being ∼0.77 eV above the lowest energy isomer **18A**. Other local minima, namely **18E**, **18F**, and **18G**, which can be considered as arising from capping one Nb atom to **17A** (**18E**, **18F**) and two Nb atoms to **16A** (**18G**), are much less stable than **18A**. These are predicted to be 1.78−3.17 eV above the ground state **18A** (see Figure S3 of the ESI).

The vibrational spectrum of **18A** (^{1}A) contains (at least) six distinct bands located in the range of 150−275 cm^{-1}, where the highest one is centered at around 260 cm^{-1}. The IR spectrum of

dx.doi.org/10.1021/jp302279j | J. Phys. Chem. A 2012, 116, 7405−7418

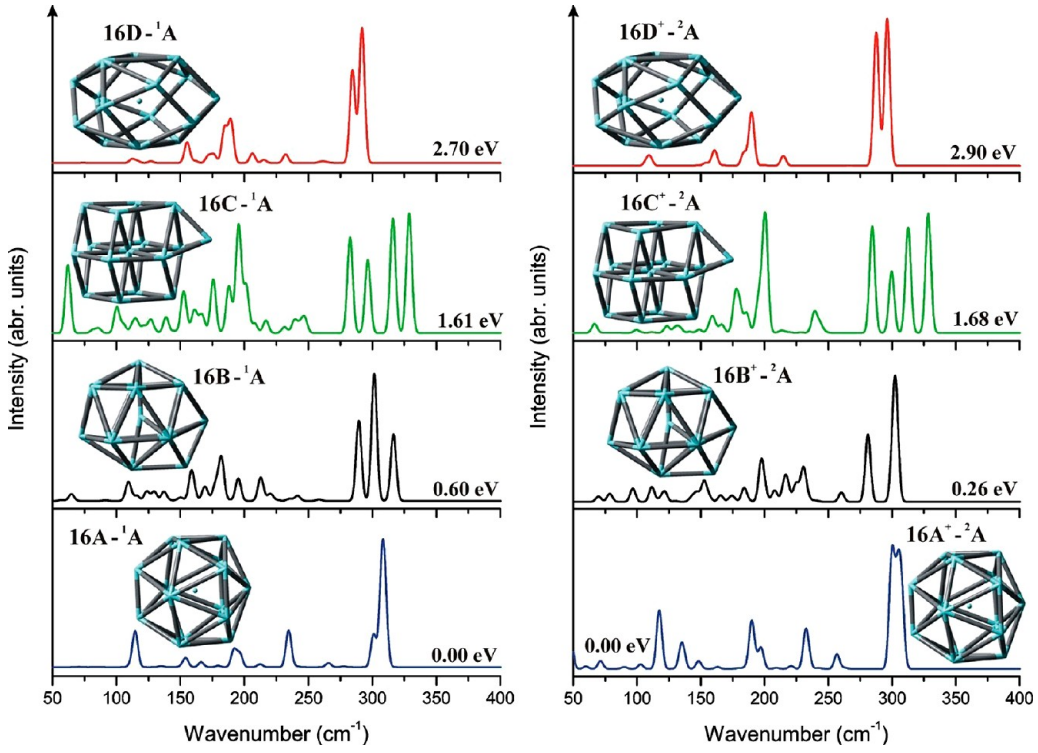

Figure 4. Predicted IR spectra of Nb_{16} neutral (left) and cation (right).

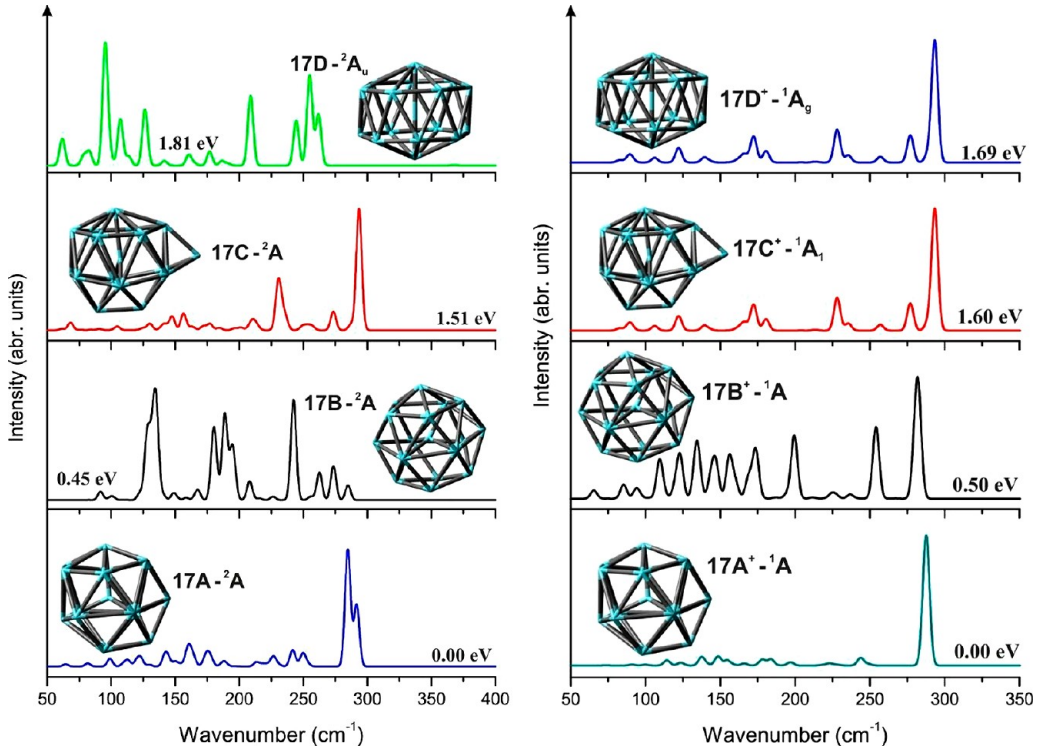

Figure 5. Predicted IR spectra of Nb_{17} neutral (left) and cation (right).

18B ($^1A_1$) is much simpler with the presence of the most intense band at ~190 cm^{-1} and a doublet at ~255 cm^{-1}. Removal of one electron from **18A** and **18B** forming **18A**$^+$ and **18B**$^+$ cations is accompanied by a significant change in the vibrational spectrum. While the intensities of bands below 225 cm^{-1} of the **18A** spectrum are significantly reduced, the doublet at ~255 cm^{-1} on the **18B** band pattern now splits into several peaks and some substantially shift to higher energy levels. The band patterns of **18A**$^-$ and **18B**$^-$ anions are also quite different from those of the corresponding neutrals and cations.

The Nonadecamers Nb_{19}. Species containing 19 atoms constitute an extensively studied object in metal clusters as the icosahedral growth pattern gives rise to a double icosahedron.[29] However, in the case of Nb_{19}, no low-lying isomer is directly

dx.doi.org/10.1021/jp302279j | J. Phys. Chem. A 2012, 116, 7405−7418

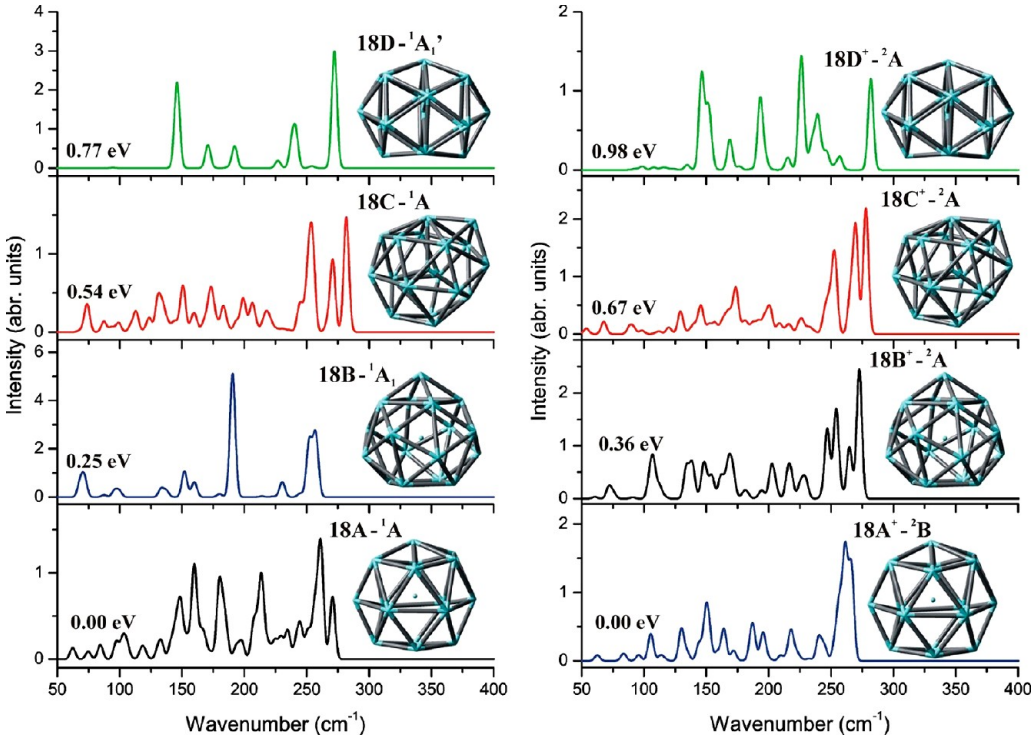

Figure 6. Predicted IR spectra of Nb_{18} neutral (left) and cation (right).

derived from a double icosahedron. Instead, it prefers a hexadecahedron-like structure **19A** (Figure 7), which is built upon **18B**. This lends support for the view that the icosahedral growth is not favored in niobium clusters. Also particularly stable is a compact structure **19B**, being only 0.04 eV higher in energy than **19A**. In **19B**, the numbers of vertices where five and six faces meet amount to 12 and 6. Another compact isomer, i.e. **19C**, with one degree 4, seven degree 5, and ten degree 6 vertices, is predicted to be 0.44 eV above **19A**. In addition, we can locate several local minima built upon the 5-fold symmetry **18D** of the smaller size by capping one Nb atom randomly. They are computed to be 1.0−2.2 eV less stable than the lowest energy isomer.

The two lowest lying structures **19A** and **19B** also turn out to be the energetically optimized configurations for both ions. The state ^1A of **19B**$^+$ is now only 0.05 eV higher in energy than its counterpart $^1A_1$ of **19A**$^+$. Both structures are thus basically degenerate. Early experiments also observed the presence of different structural isomers for cationic species Nb_{19}^+.[30] Because the cations and neutrals have similar structures, the structural isomers of the neutral Nb_{19} could exist as well, but this is also dependent on the energy barrier to their interconversion. This kinetic issue is not addressed in the present work.

Figure 7 displays the vibrational spectra of 19-atom species in both neutral and cationic states. The predicted spectrum of **19A** ($^2B_1$) contains distinct peaks in the vicinity of 110, 200, and 250 cm^{-1}, besides the appearance of a very low-frequency band below 50 cm^{-1}. The IR spectrum of the quasi-degenerate state **19B** (^2B) becomes much more complicated with the presence of (at least) seven typical bands in the range of 125−250 cm^{-1}. The vibrational spectrum of **19A**$^+$ ($^1A_1$), as in **19A**, is also characterized by recognizable peaks at around 110, 200, and 250 cm^{-1}. However, their intensities are somewhat different, and the low-frequency vibration below 50 cm^{-1} is not observed on the band pattern of **19A**$^+$.

There also exist some minor but distinguishable differences between the vibrational spectra of **19B** and **19B**$^+$. Following the electron detachment to form **19B**$^+$, the intensities of bands in the range 150−200 cm^{-1} are substantially reduced, in addition to the emergence of a distinct band at 225 cm^{-1} and a small blue shift from the peak around 125 to 135 cm^{-1}.

The Eicosamers Nb_{20}. Recently, Gruene and co-workers[31] confirmed a regular tetrahedron (T_d) as the global minimum for Au_{20} using a combined IR and computational study. On the contrary, a double icosahedron (D_{5h}) with two encapsulated atoms is predicted to be most stable form of Ni_{20},[32] whereas a face-capped octahedron (C_{3v}) is the favored form of Pd_{20}.[33] None of such conformations is found in our extensive search to be even a local minimum for Nb_{20}. Instead, the cluster has its most stable form as the polyhedron **20A**, whose degree five and six vertices are 12 and 7, respectively. Besides, we detect an isoenergetic form **20B** ($^1A'$) competing for the ground state of Nb_{20} as it is located only 0.07 eV above **20A** (^1A). The shape **20B** arises from the 5-fold symmetry structure **18D** by capping two additional Nb atoms. Both **20A** and **20B** also turn out to be the lowest and the second-lowest forms of the ions. However, the energy separation is enlarged upon ion formation, in which **20B**$^+$ and **20B**$^-$ are now 0.27 and 0.13 eV above their counterparts **20A**$^+$ and **20A**$^-$, respectively.

We now consider the vibrational properties of some lower lying states of Nb_{20} and Nb_{20}^+, which are plotted in Figure 8. The predicted spectrum of **20A** contains two distinct peaks at ∼175 and 240 cm^{-1}. In addition, the highest energy band is observed at 265 cm^{-1} and several low-intensity ones in the vicinity of 175−225 cm^{-1}. The vibrations of **20B** ($^1A'$) are characterized by two strong peaks at around 235 and 260 cm^{-1}, and some lower bands at ∼185, 145, and 75 cm^{-1}. Regarding the cation **20A**$^+$, it is similar to **20A** that one can clearly find the significant peak around 245 cm^{-1}. However, the peak at ∼175 cm^{-1} is now significantly reduced. The spectrum of **20B**$^+$ contains three

dx.doi.org/10.1021/jp302279j | J. Phys. Chem. A 2012, 116, 7405−7418

Table 2. Ground and Lower Lying States of $Nb_n^{0/\pm}$ (n = 18–20) Clusters and the Relative Energies (RE, eV, BPW91/cc-pVDZ-PP)

cluster	structure	state	RE (eV)	cluster	structure	state	RE (eV)
Nb_{18}	**18A** (C_1)	^{1}A	0.00		**19F$^+$** (C_s)	^{1}A′	1.13
	18B (C_{2v})	$^1A_1$	0.25		**19G$^+$** (C_{2v})	$^1A_1$	1.34
	18C (C_1)	^{1}A	0.54		**19H$^+$** (C_1)	^{2}A	2.41
	18D (D_{5h})	$^1A_1$′	0.77	Nb_{19}^-	**19A$^-$** (C_{2v})	$^1A_1$	0.01
	18E (C_1)	1A	1.78		**19B$^-$** (C_1)	^{1}A	0.00
	18F (C_s)	^{1}A′	2.03		**19C$^-$** (C_1)	^{1}A	0.37
	18G (D_{3h})	$^1A_1$′	3.17		**19D$^-$** (C_1)	^{1}A	0.98
Nb_{18}^+	**18A$^+$** (C_2)	^{2}B	0.00		**19E$^-$** (C_1)	^{1}A	1.25
	18B$^+$ (C_1)	^{2}A	0.36		**19F$^-$** (C_s)	^{1}A′	0.96
	18C$^+$ (C_1)	^{2}A	0.67		**19G$^-$** (C_2)	^{1}A	1.11
	18D$^+$ (C_1)	^{2}A	0.98	Nb_{20}	**20A** (C_1)	^{1}A	0.00
	18E$^+$ (C_1)	^{2}A	2.18		**20B** (C_s)	^{1}A′	0.07
	18F$^+$ (C_s)	^{2}A′	2.30		**20C** (C_1)	^{1}A	0.35
	18G$^+$ (C_1)	^{2}A	3.45		**20D** (C_s)	^{1}A′	0.36
Nb_{18}^-	**18A$^-$** (C_1)	^{2}A	0.00		**20E** (C_1)	^{1}A	0.38
	18B$^-$ (C_{2v})	$^2A_1$	0.10		**20F** (C_1)	^{1}A	0.58
	18C$^-$ (C_s)	^{2}A	0.42		**20G** (C_s)	^{1}A′	1.06
	18D$^-$ (C_1)	^{2}A	0.65		**20H** (C_1)	^{1}A	1.20
	18E$^-$ (C_1)	^{2}A	1.64	Nb_{20}^+	**20A$^+$** (C_1)	^{2}A	0.00
	18F$^-$ (C_s)	^{2}A″	1.63		**20B$^+$** (C_1)	^{2}A	0.27
	18G$^-$ (C_1)	^{2}A	2.88		**20C$^+$** (C_1)	^{2}A	0.31
Nb_{19}	**19A** (C_{2v})	$^2B_1$	0.00		**20D$^+$** (C_s)	^{2}A″	0.50
	19B (C_2)	^{2}A	0.04		**20E$^+$** (C_1)	^{2}A	0.38
	19C (C_s)	^{2}A	0.44		**20F$^+$** (C_1)	^{2}A	0.40
	19D (C_1)	^{2}A	1.00		**20G$^+$** (C_s)	^{2}A′	1.06
	19E (C_1)	^{2}A′	1.06		**20H$^+$** (C_1)	^{2}A	1.32
	19F (C_1)	^{2}A	1.20	Nb_{20}^-	**20A$^-$** (C_1)	^{2}A	0.00
	19G (C_{2v})	$^2B_1$	1.21		**20B$^-$** (C_s)	^{2}A′	0.13
	19H (C_s)	^{2}A′	2.20		**20C$^-$** (C_1)	^{2}A	0.35
Nb_{19}^+	**19A$^+$** (C_{2v})	$^1A_1$	0.00		**20D$^-$** (C_s)	^{2}A′	0.28
	19B$^+$ (C_2)	^{1}A	0.05				
	20E$^-$ (C_1)	^{2}A	0.45				
	19C$^+$ (C_1)	^{1}A	0.54		**20F$^-$** (C_1)	^{2}A	0.30
	19D$^+$ (C_1)	^{1}A	0.99		**20G$^-$** (C_s)	^{2}A″	0.73
	19E$^+$ (C_1)	^{1}A	1.16		**20H$^-$** (C_1)	^{2}A	1.01

closely spaced peaks at 255, 240, and 220 cm^{-1}, and a relatively typical one at around 150 cm^{-1}.

3.2. Energetic Properties. Some basic energetics of pure niobium clusters such as EAs and IEs have been determined experimentally by several groups.[17,18,34] Photoemission studies[17] predicted that the even-numbered clusters, namely Nb_8, Nb_{10}, Nb_{12}, Nb_{14}, and Nb_{16}, have a closed-shell structure and that the additional electron occupies the LUMO, giving rise to a small peak at low binding energy of the corresponding anions. Exceptionally large frontier orbital (HOMO–LUMO) energy gaps found for 8-, 10-, and 16-atom neutral species correlate well with experiments, that is, the reactivity of these clusters with H_2, N_2, and CO is abnormally low as compared to other counterparts.[12,13] In our recent study,[7] the relation of large orbital gaps to low reactivities has been interpreted for Nb_8 and Nb_{10} through the chemical index, i.e., the *global hardness* ($\eta \approx$ IE − EA),[35] in which a "hard" cluster should be less reactive. As far as we are aware, there is no theoretical data reported for both EAs and IEs of Nb_n containing more than 12 atoms.

We here systematically evaluate the vertical and adiabatic detachment energies for $Nb_n^{0/-}$ species in the range of size n = 13–20, using the same BPW91/cc-pVDZ-PP level. The vertical detachment energies (VDEs) of anions are calculated at the anion geometry, whereas the adiabatic detachment energies (ADEs) refer to the values obtained by using the optimized structures of both neutral and anionic forms. The latter qualities also correspond to the EAs of neutral clusters. Similarly, we compute the vertical and adiabatic detachment energies of neutrals, which correspond to the vertical and adiabatic IEs. The vertical IEs of neutrals are thus computed by taking the geometries of vertical cations to be the same as those of neutral counterparts, while the adiabatic ionization energies are computed from the difference between the energies of both neutral and cationic ground states. Table 3 lists, along with available experimental data, the vertical and adiabatic values for both EAs and IEs of the $Nb_n^{0/-}$ clusters considered.

The even/odd oscillations of IEs and EAs are typically found in small metal clusters bearing an odd number of electrons per atom such as Na, Al, and Au,[1,36,37] and also are Nb clusters smaller than Nb_{12}. For Nb_n^- species with n = 13–17, such a pattern of the VDEs is again observed with local minima at n = 14 and 16, while for n > 17 the VDEs tend to increase steeply with no clear even/odd alternation. These results concur with the experimental data estimated from the photoelectron spectra of mass-separated Nb_n^- clusters.[17]

We also find that, in general, the detachment energies calculated from the lowest energy structures are in substantially better agreement with experiment than those obtained from higher energy isomers. For example, the predicted ADEs of **13A$^-$** and **13B$^-$** are 1.68 and 1.48 eV, respectively, as compared to the experimental value of 1.70 eV. Only in the case of Nb_{18}^- a low-lying structure **18B$^-$** yields a closer VDE to experiment (see Table 3), although it is computed to lie ∼0.25 eV above the ground state.

Kietzmann et al.[17] suggested a considerable change in the electronic structure and also the atomic arrangement around n = 16 as the photoelectron spectrum of Nb_{15}^- shows a peculiar landscape, and for n > 15 the VDEs start to increase considerably with cluster size. A possible reason for such observations is that Nb clusters favor solid bcc structures with the first geometric shell closing occurring at n = 15. In this work, we find that the preferred 15-atom capped cube actually corresponds to a piece of bcc bulk with one Nb atom encapsulated by a rhombic dodecahedron shell. The unambiguous evidence for such early transition to a bulk structure also indicates that these metallic

dx.doi.org/10.1021/jp302279j | J. Phys. Chem. A 2012, 116, 7405–7418

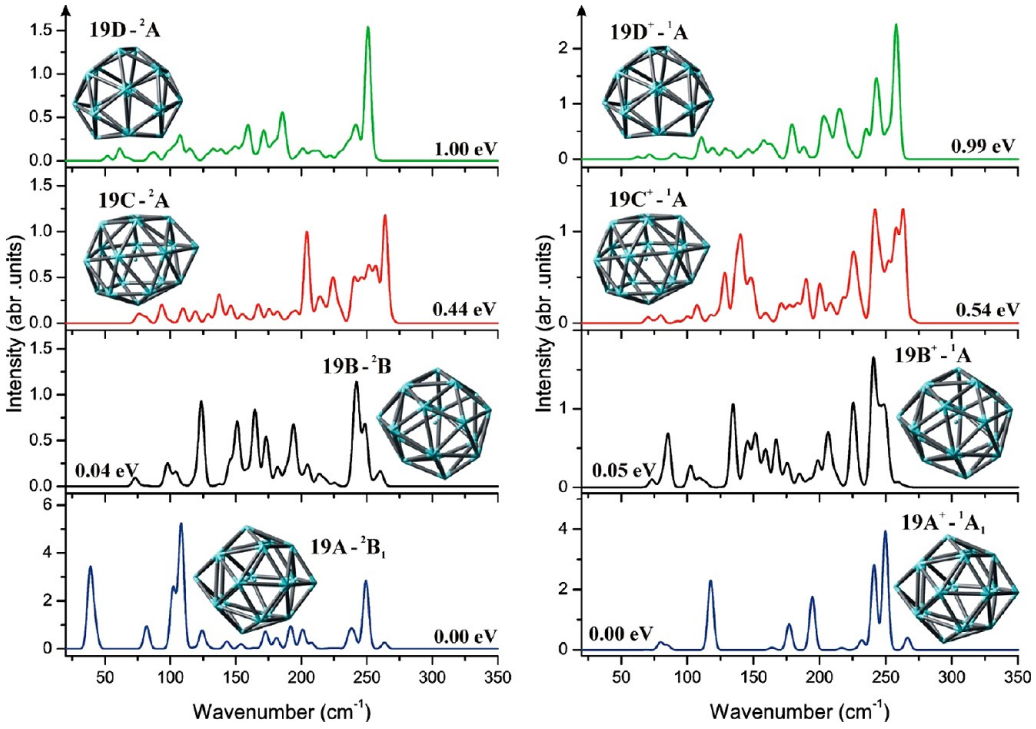

Figure 7. Predicted IR spectra of Nb_{19} neutral (left) and cation (right).

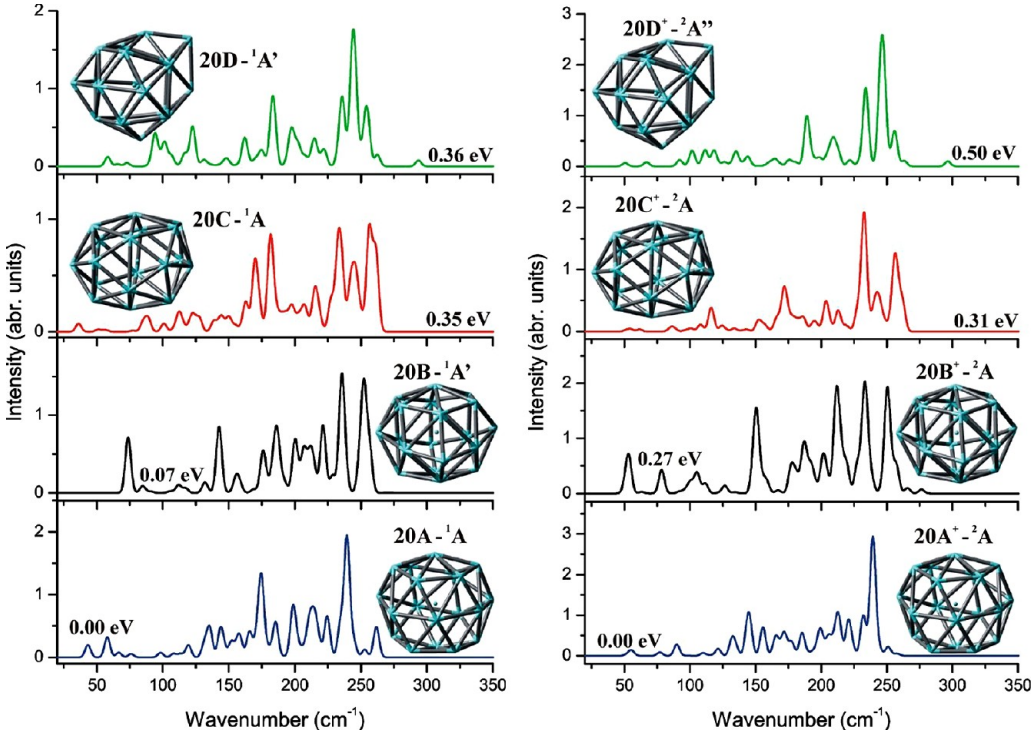

Figure 8. Predicted IR spectra of Nb_{20} neutral (left) and cation (right).

clusters are strongly bound. The Nb_{15}^- anion is in addition computed to have a detachment energy much larger than any other cluster considered, implying that it is remarkably stable with respect to neutralization.

At the BPW91/cc-pVDZ-PP level, the VDE(Nb_{15}^-) amounts to ~2.04 eV as compared to 1.68, 1.60, 1.54, 1.63, 1.81, 1.75, and 1.80 eV of Nb_{13}^-, Nb_{14}^-, Nb_{16}^-, Nb_{17}^-, Nb_{18}^-, Nb_{19}^-, and Nb_{20}^-, correspondingly. The calculated VDE of 2.04 eV for Nb_{15}^- thus significantly overestimates the experimental values of 1.65 eV by Kietzmann et al.[18] or 1.79 eV by Pramann et al.[38] On the contrary, the computed VDEs of Nb_{17}^-, Nb_{19}^-, and Nb_{20}^- tend to be 0.1−0.2 eV lower than the experiment. It is in addition noticeable that the gap separating the vertical and adiabatic EA(Nb_{15}^-) is the largest, due to the significant difference between the lowest energy structures of Nb_{15}^- and Nb_{15}.

dx.doi.org/10.1021/jp302279j | J. Phys. Chem. A 2012, 116, 7405−7418

Table 3. Ionization Energies of Nb_n and Detachment Energies of Nb_n^- (n = 13−20) (BPW91/cc-pVDZ-PP)

	ionization energies (eV)			detachment energies (eV)		
isomer	AIEs	VIEs	exptl (±0.05)[a]	ADEs	VDEs	exptl (±0.05)[b]
13A	4.70	4.76	4.85	1.66	1.68	1.70
13B	4.47	4.50	4.85	1.44	1.48	1.70
14A	4.59	4.72	4.75	1.56	1.60	1.64
15A	4.60	4.65	4.53	1.93	2.04	1.65
16A	4.54	4.66	4.80	1.48	1.54	1.62
17A	4.43	4.48	4.67	1.58	1.63	1.80
18A	4.36	4.41	4.65	1.62	1.65	1.80
18B	4.47	4.56	4.65	1.77	1.81	1.80
19A	4.37	4.40	4.63	1.65	1.75	1.88
19B	4.42	4.50	4.63	1.66	1.70	1.88
20A	4.43	4.45	4.62	1.77	1.80	1.93
20B	4.60	4.64	4.62	1.72	1.73	1.93

[a]Taken from ref 18. [b]Taken from ref 17.

Knickelbein and Yang[18] assigned the IEs for clusters up to Nb_{76} from the corresponding photoionization efficiency (PIE) spectra. Such thermochemical parameters for systems in the size range n = 4−200 were also reported by Wrigge and co-workers in a more recent paper.[34] However, to our best knowledge, theoretical calculations have only been performed for sizes up to n = 12 so far. We now report both vertical and adiabatic IEs for species with n = 13−20. The calculated results, along with the experimental data, are listed in Table 3. It appears that the experimental IEs correspond to the vertical values, and as in the detachment energies, the best match to experiment is generally related to the lowest energy structures, except for Nb_{18}. In the latter case, the calculated VIEs of **18A** and **18B** are 4.41 and 4.56 eV, respectively, as compared to the experimental value of 4.65 eV.[18] The VIEs computed from the low-lying isomers **19B** and **20B** also match better with experimental data. In both cases the energy difference between those isomers and the ground state is extremely small, and within the expected accuracy of the DFT methods (see above), they are energetically degenerate. In these cases, the higher energy isomer identified by DFT computations could legitimately be considered as the observed structure in the experiment.

Although there exists a clear odd−even oscillation of IEs for clusters smaller than Nb_{12},[7] such a pattern is not obviously observed for the larger size range n = 13−20. In agreement with experiment, the 13-atom cluster is computed to have the largest IE value. Other local maxima appear at n = 14 and 16. In general, the VIEs computed at the BPW91/cc-pVDZ-PP level compare well to experiment but with some exceptions. According to Knickelbein and Yang,[18] Nb_{15} has a lower VIE (by ∼0.27 eV) than Nb_{16}. However, our calculations yield comparable values for both sizes. The predicted IE(Nb_{15}) = 4.65 eV is thus likely overestimated, while that of Nb_{16} (4.66 eV) underestimates the measured data. The computed IE(Nb_{17}) = 4.48 eV also appears to underestimate the experimental value of 4.67 eV, even though the deviation still lies within the expected error bars of ±0.3 eV.

Of the clusters considered, the 18-atom cluster appears remarkable as both VIE and VDE values obtained from the higher lying isomer **18B** are closer to the experimental data than those computed from the lowest energy **18A**. As stated above, it can be expected that **18B** of Nb_{18} is more likely to be present in experiments than **18A**. Previously, such a phenomenon was also recorded for Nb_6 and Nb_{12}.[7] This finding again points out that in many sizes, the global minimum cannot be assigned solely by DFT computations.

3.3. Thermodynamic Stabilities. To obtain more quantitative information about the cluster stability, we consider the average binding energy per atom (BE), the second-order difference of energy (Δ^2E), and the stepwise dissociation energy D_e. For pure niobium clusters, these parameters are defined by the following equations:

$$\mathrm{BE}(\mathrm{Nb}_n^x) = [(n-1) \times E(\mathrm{Nb}) + E(\mathrm{Nb}^x) - E(\mathrm{Nb}_n^x)]/n$$

$$\Delta^2E(\mathrm{Nb}_n^x) = E(\mathrm{Nb}_{n+1}^x) + E(\mathrm{Nb}_{n-1}^x) - 2E(\mathrm{Nb}_n^x)$$

$$D_e(\mathrm{Nb}_n^x) = E(\mathrm{Nb}_{n-1}^x) + E(\mathrm{Nb}) - E(\mathrm{Nb}_n^x)$$

where x = 0, +1, −1; $E(\mathrm{Nb}_n^x)$ is the lowest energy of the Nb_n^x cluster.

The computed BEs for neutral species and their singly charged counterparts calculated at various levels are given in Table 4. Such parameter can be regarded as the energy gained in assembling a definite cluster from isolated Nb constituents. First we find a monotonic increase of BEs with respect to the cluster sizes. This implies that the systems tend to gain stability during the growth; larger clusters are indeed more stabilized. As reported in our previous studies,[7] although the BPWP1 functional is in general more reliable than other functionals in predicting geometries, vibrations and energetics of Nb clusters, it is deficient when computing the binding energy per atom and dissociation energies. For the latter, the hybrid meta-GGA functional M06 describes somewhat better. The biggest drawback of most GGA approaches is the evaluation of the atomic energies,[39] and as a consequence, quantities involving the energies of free atoms become less relevant. For the sake of

Table 4. Average Binding Energy Per Atom (BE), Second-Order Difference of Energy (Δ^2E), and Dissociation Energy (D_e) of $Nb_n^{0/+}$ Clusters (n = 13−20), Using BPW91 and M06 Functionals with the cc-pVDZ-PP Basis Set

	neutral clusters						cationic clusters					
	BE (eV)		D_e (eV)		Δ^2E (eV)		BE (eV)		D_e (eV)		Δ^2E (eV)	
n	BPW91	M06	BPW91	M06	BPW91	M06	BPW91	M06	BPW91	M06	BPW91	M06
13	4.67	5.14	4.93	5.85	−1.22	−0.68	4.87	5.28	4.77	5.42	−1.67	−1.14
14	4.78	5.25	6.15	6.64	−0.41	−0.33	4.96	5.37	6.13	6.56	−0.34	−0.54
15	4.90	5.36	6.56	6.97	1.38	0.94	5.06	5.49	6.47	7.01	1.13	1.09
16	4.91	5.41	5.20	6.03	−0.20	0.28	5.08	5.52	5.34	6.01	−0.16	0.08
17	4.94	5.43	5.40	5.75	0.17	0.22	5.10	5.54	5.50	5.93	0.21	0.35
18	4.95	5.43	5.22	5.53	−0.06	−0.17	5.11	5.55	5.29	5.58	0.02	−0.13
19	4.97	5.44	5.28	5.69	1.13	1.10	5.12	5.56	5.28	5.71	1.22	1.88
20	4.93	5.40	4.15	4.60			5.07	5.52	4.10	4.55		

dx.doi.org/10.1021/jp302279j | J. Phys. Chem. A 2012, 116, 7405−7418

comparison, we here report both M06 and BPW91 values for these quantities.

The cations are predicted to have larger BEs than the corresponding neutrals by both functionals (Table 4). In addition, the BPW91 systematically yields lower BE values than the M06, with the average deviations of ~0.5 and ~0.4 eV for neutral and cationic states, respectively. The BEs of clusters considered are predicted to be in the range of 4.7−5.0 eV/atom by BPW91, as compared to the corresponding values of 5.1−5.4 eV/atom computed using the M06. The BEs thus exhibit a gradual growth and tend to reach the maximal value of 5.4 eV/atom for Nb_{19} (M06 level). However, this quantity is still far away from the cohesive energy of the bulk niobium (7.6−7.8 eV/atom).[40] While measured values were reported for neutrals smaller than Nb_{12},[41] no experimental data are found for the larger clusters.

The time-of-flight (TOF) mass spectra of Nb clusters recorded by Sakurai et al.[42] show a remarkably high intensity for the systems in the range of n = 11−16. Subsequently the intensity significantly decreases and reaches a minimum at n = 19. This observation correlates well with the dissociation energy D_e values tabulated in Table 4. Indeed, the predicted values for clusters with n = 13−16 are much higher than those of the larger systems. Especially, both Nb_{15} and Nb_{15}^+ are expected to be exceptionally stable as they exhibit the especially large D_e values. Among the neutrals considered, Nb_{15} is characterized by the highest D_e value, implying a particular thermodynamic stability even though it has an open-shell electronic structure. These results indicate again the dominance of a *geometric effect*, namely the cluster stability is determined more by the atomic arrangement (shape) than by the electron distribution.

The magic number of n = 15 was found for the pure clusters of Fe, Ti, Zr, and Ta, owing to their bcc structural unit.[42] In addition, both Fe_{19} and Ti_{19} were also assigned to be magic as they are expected to hold a highly symmetric conformation, i.e., a double icosahedron with two encapsulated atoms. The 19-Nb atom species, on the contrary, does not prefer such a form because, as compared to 3d elements, the 4d elements have larger volume in such a way that the 5-fold symmetry cage of 17-Nb atoms can conveniently encapsulate two Nb atoms. This concurs with the low intensity on the abundance spectra of autoionized Nb clusters observed by Sakurai et al. for Nb_{19}.[42]

As far as we are aware, no experimental dissociation energies are actually available for clusters containing more than 11 Nb atoms. We recently used both M06 and BPW91 functionals to predict dissociation energies, and the former is found to yield a better agreement with experiment than the latter.[7] In this context, we would suggest to adopt the D_e values predicted by the M06 level for Nb_n in the range of n = 13−20.

Another indicator that can be used to estimate the relative stability of a cluster with respect to its immediate neighbors is the second-order difference of energy (Δ^2E). A cluster with a positive value of Δ^2E is considered to be more stable as compared to the smaller and larger size neighbors. At both levels (Table 4), the 15-atom species are found to have the largest values of Δ^2E, indicating their higher stabilities. This is again in perfect agreement with the analysis based on dissociation energies given above. For smaller systems, the Δ^2Es clearly exhibit odd−even fluctuations: clusters with an even number of atoms appear to be much more stable than the neighboring odd-numbered ones.[7] However, such a trend is not observed for the systems considered here.

The energy gap between frontier orbitals (HOMO−LUMO) is also used to measure the kinetic stability of chemical species. The relatively large HOMO−LUMO gaps of Nb_8, Nb_{10}, and Nb_{16} that were estimated from photoelectron spectra of the corresponding anions are found to correlate well with their low reactivities toward hydrogen (Figures 9−11).[17] Low reactivities

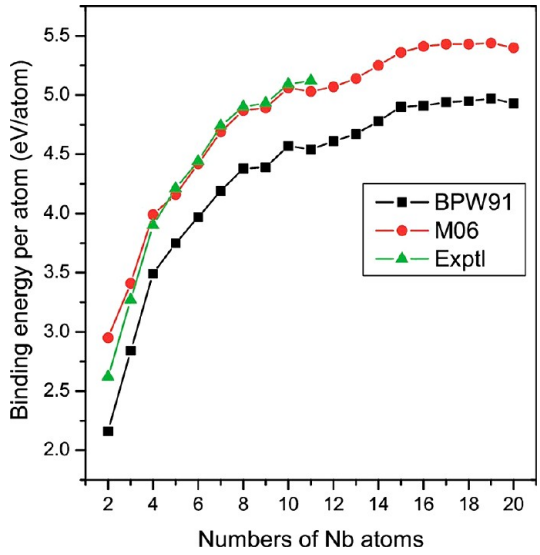

Figure 9. Binding energies per atom for the neutral Nb clusters vs cluster size. The experimental values are taken from ref 41.

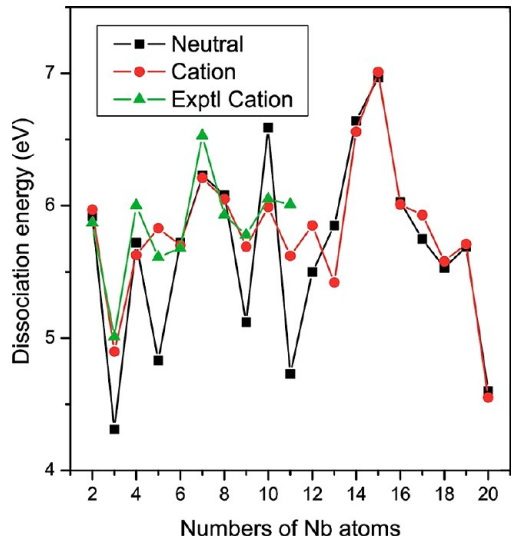

Figure 10. Dissociation energies for Nb_n clusters in both neutral and cationic states as a function of cluster sizes. The experimental values are taken from ref 41.

toward nitrogen and deuterium were also detected experimentally for these clusters.[12] The graph of the HOMO−LUMO gaps for the lowest energy structures of neutral and cationic Nb clusters is given in Figure 9. Because such separations of the closed-shell systems and the SOMO-LUMO gaps of the open-shell radicals cannot directly be compared, we only plot the gaps for closed-shell species. This clearly demonstrates that Nb_{16} has the largest band gap among neutrals considered. Concerning the cations, the large gap obtained for Nb_{15}^+ correlates with its high stability discussed above. However, its reactivity with simple

dx.doi.org/10.1021/jp302279j | J. Phys. Chem. A 2012, 116, 7405−7418

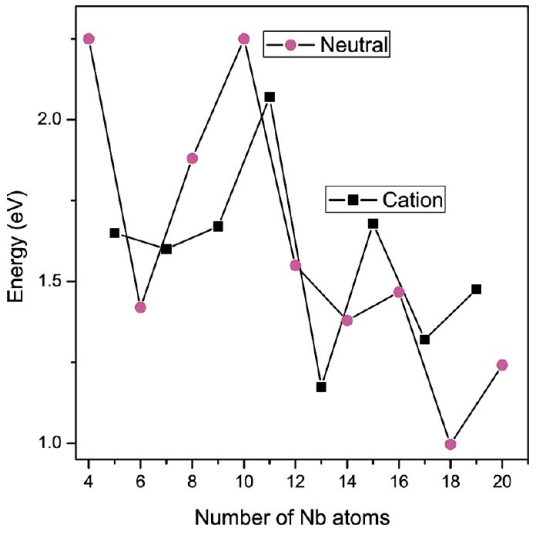

Figure 11. Evolution of HOMO−LUMO gaps with respect to cluster size for neutral and cationic Nb_n clusters.

molecules in the gas phase is comparable to that of other Nb cationic clusters.[15,16,43]

In order to probe further the high stability of some specific sizes, the shapes and symmetries of MOs generated from interactions between valence orbitals of the encapsulated Nb atoms with the outside niobium frameworks in Nb_{15}^- and Nb_{19}^- systems are displayed in Figure 12. Such combinations are analogous to those of the homoleptic complexes in which the encapsulated Nb serves a function of the central atom whose

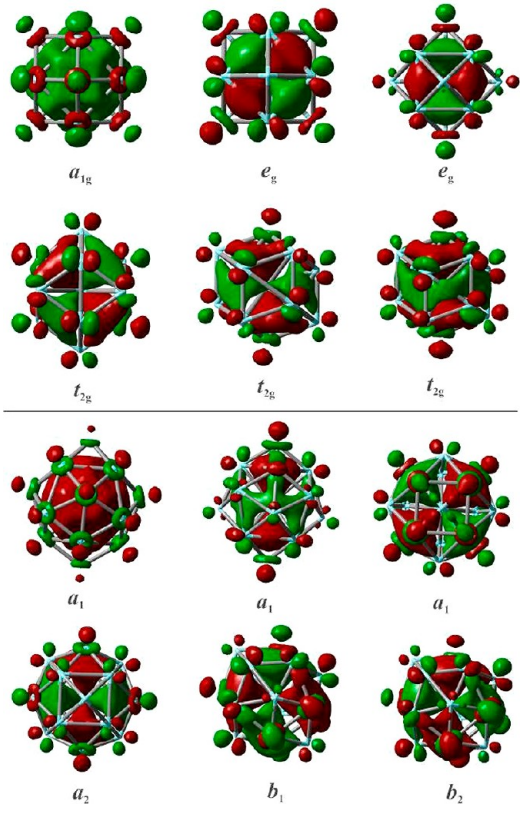

Figure 12. Shapes and symmetries of MOs generated from valence orbitals of central Nb in Nb_{15}^- (upper panel) and Nb_{19}^- (lower panel).

benefit is a stabilizing effect for Nb cages. When placed at the center of an Nb_{14} cube, five d orbitals of Nb are no longer degenerate (Figure 12). Instead they split into two nonequivalent sets of orbitals with e_g and t_{2g} subsymmetries of the O_h group. Similar interactions are also observed in larger systems such as Nb_{19}^-. However, in the latter, five d orbitals split into five discrete levels 2 a_1, a_2, b_1, and b_2 of the C_{2v} point group. Furthermore, moving to Nb_{19}^-, the Nb_{18} skeleton expands, so linear combinations of encapsulated Nb valence orbitals with those of the Nb_{18} cage become less effective. This is likely to result in a greater stabilization of the pentadecamers, as compared to other species considered in the present work. In addition, we find an electron density flow from the outside Nb atoms to the encapsulated one as the net charges of the latter moiety are consistently negative (see Table 5). The incomplete d

Table 5. The Natural Charges Distributed on the Encapsulated Nb Atom of Nb_n Clusters (n = 13−20) (BPW91/cc-pVDZ-PP)

isomers	NBO charges (au)	isomers	NBO charges (au)
13A	−1.3	**18A**	−1.1
13B	−1.0	**18B**	−1.2
14A	−1.1	**19A**	−1.2
15A	−1.5	**19B**	−1.0
16A	−1.3	**20A**	−1.0
17A	−1.2	**20B**	−1.1

orbitals of the central atom thus basically play as a global electron acceptor. As expected, the electron transfer in **15A** is much more effective as compared to the similar procedure in other species. Therefore, it can be suggested that the greater the charge involved, the more stabilized the cluster is.

Figure 13 displays the density of states (DOS) of the lowest energy isomers **14A**$^-$, **15A**$^-$, and **16A**$^-$. The occupied densities of states of these systems are predicted to cover the range from −1.0 to −6.0 eV, and all associated mainly with 4d and 5s electrons. The photoemission spectra for these anions have also been investigated by several experimental groups,[17,34] and that of Nb_{15}^- is found to be particular with sharper peaks in the vicinity of 2.5−3.0 eV, along with some minor intensities around 2.0 eV. This is in general agreement with our results, though the computed data are likely to be shifted to lower binding energies as compared to the photoemission peaks. A simulation of the PE spectrum requires computations of the Franck−Condon factors, and a rough direct comparison of the electronic density of states with the PE spectra is often carried out.[44] However, it should be noticed that such an approach is only of qualitative value for assignment of cluster geometries as it does not take the relaxation of the electrons into account.[45]

4. CONCLUDING REMARKS

In this theoretical study, we perform a comprehensive investigation on the structures and related properties of niobium clusters in the range from 13 to 20 atoms, in three different charged states, using the BPW91 functional and the pseudopotential basis set cc-pVDZ-PP. The M06 functional is also employed to evaluate some basic thermochemical parameters including atomization and dissociation energies. Together with the results obtained in our recent studies on smaller clusters,[7] we can now draw some general trends for Nb_n with n ranges from 2 to 20.

dx.doi.org/10.1021/jp302279j | J. Phys. Chem. A 2012, 116, 7405−7418

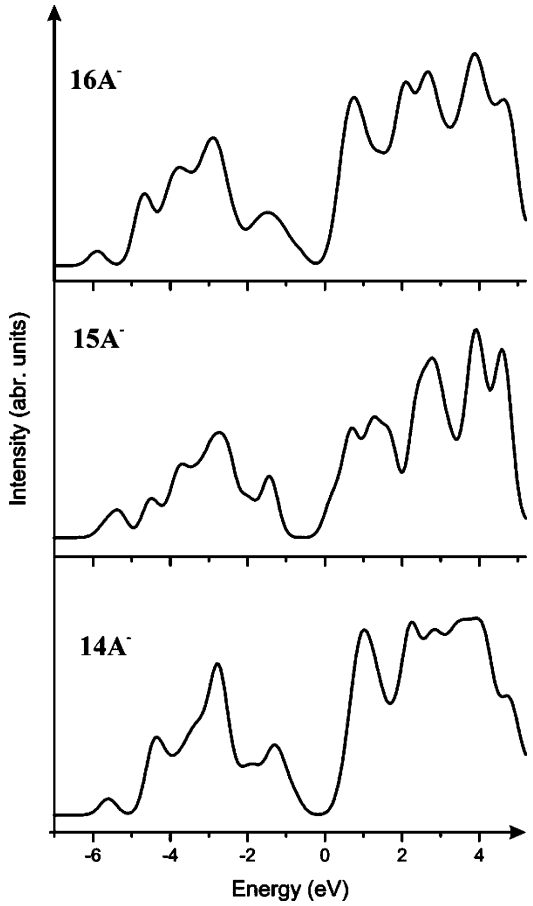

Figure 13. Plots of total density of states (DOS) for anions **14A**$^-$, **15A**$^-$, and **16A**$^-$.

The Nb clusters invariably prefer the lowest possible spin state for their ground state, i.e., singlet and doublet states for even- and odd-electron systems, respectively. We also find that, in terms of their growth, these clusters do not favor an icosahedral evolution. Instead, they consistently follow the path in which a compact structure with one Nb atom encapsulated by a cage is formed from five and six triangles. Unlike many 3d transition metals whose volumes are much smaller, the clusters containing 13 and 19 Nb atoms are not likely to exist as icosahedra and double-icosahedra. A distinct case is Nb_{15} as its capped cube bears a slightly distorted solid bcc structure.

In some cases, we also observe for a certain system several lower lying isomers that are very close in energy, in such a way that sole DFT computations cannot clearly establish their ground electronic states. The present computed results confirm the existence of structural isomers with comparable energy content for species with n = 13, 18, 19, and 20 in both neutral and charged states. Thus additional spectroscopic information is necessary for more reliable assignments of the global minima.

In addition to the structural predictions, we calculate the vibrational signatures. An interesting observation is that while the IR spectra of smaller systems are found to be strongly dependent on the addition or removal of an electron from the neutral, those of the larger size clusters are likely to be independent of the charged states. The neutrals and their corresponding ions usually have quite similar IR patterns.

We in addition determine the electron affinities, ionization energies, average binding energies, dissociation energies, and frontier orbital energy gaps. The computed EAs and IEs are generally in fair agreement with experiment. On the basis of the analyses of these energetic parameters, the Nb_{15} system is predicted to be stable and it can form a highly symmetric structure in all charged states.

■ ASSOCIATED CONTENT

Supporting Information

Cartesian coordinates of the optimized structures of the clusters considered. This material is available free of charge via the Internet at http://pubs.acs.org.

■ AUTHOR INFORMATION

Corresponding Author

*E-mail: minh.nguyen@chem.kuleuven.be.

Notes

The authors declare no competing financial interest.

■ ACKNOWLEDGMENTS

We are indebted to the KU Leuven Research Council for continuing support via the GOA, IDO, and IUAP programs. P.V.N. is grateful to the University of Can Tho for a partial doctoral scholarship. M.T.N. thanks the ICST for supporting his stays in Vietnam.

■ REFERENCES

(1) De Heer, W. A. *Rev. Mod. Phys.* **1993**, *65*, 611−676.
(2) Schmid, G. *Adv. Eng. Mater.* **2001**, *3*, 737−743.
(3) Goodwin, L.; Salahub, D. R. *Phys. Rev. A* **1993**, *47*, R774−R777.
(4) Gronbeck, H.; Rosen, A.; Andreoni, W. *Phys. Rev. A* **1998**, *58*, 4630−4636.
(5) Moro, R.; Yin, S.; Xu, X.; De Heer, W. A. *Phys. Rev. Lett.* **2004**, *93*, 086803.
(6) Kumar, V.; Kawazoe, Y. *Phys. Rev. B* **2002**, *65*, 125403.
(7) (a) Nhat, P. V.; Ngan, V. T.; Nguyen, M. T. *J. Phys. Chem. C* **2010**, *114*, 13210−13218. (b) Nhat, P. V.; Ngan, V. T.; Tai, T. B.; Nguyen, M. T. *J. Phys. Chem. A* **2011**, *115*, 3523−3535. (c) Nhat, P. V.; Ngan, V. T.; Tai, T. B.; Nguyen, M. T. *J. Phys. Chem. A* **2011**, *115*, 14127−14128.
(8) Hamrick, Y.; Taylor, S.; Lemire, G. W.; Fu, Z. W.; Shui, J. C.; Morse, M. D. *J. Chem. Phys.* **1988**, *88*, 4095−4098.
(9) Asmis, K. R.; Fielicke, A.; von Helden, G.; Meijer, G. The Chemical Physics of Solid Surfaces. In *Atomic Clusters: From Gas Phase to Deposited*; Woodruff, D. P., Ed.; Elsevier: Amsterdam, The Netherlands, 2007; Vol. *12*, pp 327−375.
(10) Fielicke, A.; Ratsch, C.; Von Helden, G.; Meijer, G. *J. Chem. Phys.* **2007**, *127*, 234306.
(11) Fielicke, A.; Meijer, G. *J. Phys. Chem. A* **2011**, *115*, 7869−7870.
(12) Berces, A.; Hackett, P. A.; Lian, L.; Mitchell, S. A.; Rayner, D. M. *J. Chem. Phys.* **1998**, *108*, 5476−5490.
(13) Holmgren, L.; Andersson, M.; Rosen, A. *Surf. Sci.* **1995**, *231*, 331−333.
(14) Berg, C.; Schindler, T.; Niedner-Schatteburg, G.; Bondybey, V. E. *J. Chem. Phys.* **1995**, *102*, 4870−4884.
(15) Berg, C.; Schindler, T.; Kantlehner, M.; Niedner-Schatteburg, G.; Bondybey, V. E. *Chem. Phys.* **2000**, *262*, 143−149.
(16) Pfeffer, B.; Jaberg, S.; Niedner-Schatteburg, G. *J. Chem. Phys.* **2009**, *131*, 194305.
(17) (a) Kietzmann, H.; Morenzin, J.; Bechthold, P. S.; Ganteför, G.; Eberhardt, W.; Yang, D. S.; Hackett, P. A.; Fournier, R.; Pang, T.; Chen, C. *Phys. Rev. Lett.* **1996**, *77*, 4528−4531. (b) Kietzmann, H.; Morenzin, J.; Bechthold, P. S.; Gantefor, G.; Eberhardt, W. *J. Chem. Phys.* **1998**, *109*, 2275−2278.
(18) Knickelbein, M. B.; Yang, S. *J. Chem. Phys.* **1990**, *93*, 1476−1477, and 5760−5767.
(19) Frisch, M. J.; Schlegel, H. B.; Scuseria, G. E.; Robb, M. A.; Cheeseman, J. R.; Montgomery, J. A., Jr.; Vreven, T.; Kudin, K. N.;

Burant, J. C.; Millam, J. M. et al. *Gaussian 09*, Revision: B.01; Gaussian, Inc.: Wallingford, CT, 2009.
(20) (a) Becke, A. D. *Phys. Rev. A* **1988**, *38*, 3098−3100. (b) Perdew, J. P.; Wang, Y. *Phys. Rev. B* **1992**, *45*, 13244−13249.
(21) Hay, P. J.; Wadt, W. R. *J. Chem. Phys.* **1985**, *82*, 299−310.
(22) Peterson, K. A. *J. Chem. Phys.* **2003**, *119*, 11099−11112.
(23) Jug, K.; Zimmermann, B.; Calaminizi, P.; Kçster, A. *J. Chem. Phys.* **2002**, *116*, 4497−4507.
(24) Sun, Y.; Fournier, R.; Zhang, M. *Phys. Rev. A* **2009**, *79*, 043202.
(25) Kumar, V. *Comput Mater. Sci.* **2006**, *35*, 375−381.
(26) King, R. B. *Inorg. Chim. Acta* **1995**, *235*, 111−115.
(27) Besley, N. A.; Johnston, R. L.; Stace, A. J.; Uppenbrink, J. *Theor. Chim. Acta* **1995**, *341*, 75−90.
(28) Hearn, J. E.; Johnston, R. L. *J. Chem. Phys.* **1997**, *107*, 4674−4687.
(29) Lloyd, L. D.; Johnston, R. L. *J. Chem. Soc., Dalton Trans.* **2000**, *3*, 307−316.
(30) Elkind, J. L.; Weiss, F. D.; Alford, J. M.; Laaksonen, R. T.; Smalley, R. E. *J. Chem. Phys.* **1988**, *88*, 5215−5224.
(31) Gruene, P.; Rayner, D. M.; Redlich, B.; van der Meer, A. F. G.; Lyon, J. T.; Meijer, G.; Fielicke, A. *Science* **2008**, *321*, 674−676.
(32) Song, W.; Lu, W. C.; Zang, Q. J.; Wang, C. Z.; Ho, K. M. *Int. J. Quantum Chem.* **2012**, *112*, 1717−1724.
(33) Zhang, H.; Tian, D.; Zhao, J. *J. Chem. Phys.* **2008**, *129*, 114302.
(34) Wrigge, G.; Hoffmann, M. A.; Von Issendorff, B.; Haberland, J. *Eur. Phys. J. D* **2003**, *24*, 23−26.
(35) Geerlings, P.; De Proft, F.; Langenaeker, W. *Chem. Rev.* **2003**, *103*, 1793−1873.
(36) Cha, C. Y.; Gantefor, G.; Eberhardt, W. *J. Chem. Phys.* **1994**, *100*, 995−1010.
(37) Häkkinen, H.; Landman, U. *Phys. Rev. B* **2000**, *62*, R2287−R2290.
(38) Pramann, A.; Koyasu, K.; Nakajima, A.; Kaya, K. *Int. J. Mass Spectrom.* **2003**, *229*, 77−82.
(39) Rappoport, D.; Crawford, N. R. M.; Furche, F.; Burke, K. *Computational Inorganic and Bioinorganic Chemistry*; Solomon, E. I., King, R. B., Scott, R. A., Eds.; Wiley, John & Sons, Inc.: Hoboken, NJ, 2009.
(40) Gronbeck, H.; Rosen, A. *Phys. Rev. B* **1996**, *54*, 1549−1552.
(41) Hales, D. A.; Lian, L.; Armentrout, P. B. *Int. J. Mass Spectrom. Ion Processes* **1990**, *102*, 269−301.
(42) Sakurai, M.; Watanabe, K.; Sumiyama, K.; Suzuki, K. *J. Chem. Phys.* **1999**, *111*, 235−238.
(43) Wu, Q.; Yang, S. *Int. J. Mass Spectrom.* **1999**, *184*, 57−65.
(44) Iseda, M.; Nishio, T.; Han, S. Y.; Yoshida, H.; Terasaki, A.; Kondow, T. *J. Chem. Phys.* **1997**, *106*, 2182−2187.
(45) Gronbeck, H.; Rosen, A. *J. Chem. Phys.* **1997**, *107*, 10620−10626.